J. Inst. Eng. India Ser. D (January–June 2022) 103(1):203–216
https://doi.org/10.1007/s40033-021-00322-w

ORIGINAL CONTRIBUTION

Influence of Graphene Addition on Microstructure and Mechanical Properties of Homogenized Al4032–Graphene Composites Processed Through ECAP

R. Sivarama Krishnarao[1] · V. Veeranna[2] · A. Gopala Krishna[1]

Received: 30 August 2021 / Accepted: 29 November 2021 / Published online: 26 March 2022

Abstract In the present work, an Al4032 alloy reinforced with various contents of graphene (0, 1, 3, 5 wt.%) was fabricated via stir casting and an 8 h homogenization process. The Al4032–graphene composites were severely deformed by equal channel angular pressing (ECAP). The microstructure and fractography of composites at different processing stages have been investigated using optical microscopy and scanning electronic microscopy. The results reveal that the graphene sheets were dispersed homogeneously and Al4032 matrix grains were significantly refined with ECAP process. Moreover, the agglomeration of reinforcement with the addition of 3% and 5% of graphene in matrix alloy is also refined and bounded in the grain boundaries. The composites mechanical properties were assessed as a function of the number of passes in ECAP process. After 6 runs of ECAP, the hardness and tensile characteristics of the material improved considerably.

Keywords Aluminium composite · Graphene · ECAP · Homogenization · Mechanical properties

✉ R. Sivarama Krishnarao
rskrishnarao0@gmail.com

[1] Department of Mechanical Engineering, University College of Engineering, JNTUK, Kakinada 533003, India

[2] Department of Mechanical Engineering, St. Johns Engineering College, Yemmiganur 518360, India

Introduction

Aluminium alloys and their composites have attracted for many researchers due to their light weight, reasonable cost and superb ductility [3, 11, 37]. Carbon-based elements are the perfect reinforcements for many of the composite materials due to their remarkable combination of mechanical and thermal properties [33, 34]. Because of low-density requirements in aerospace and auto-industry, traditional reinforcements like fibres and ceramics cannot satisfy the need [15, 16]. Graphene is a single-atom thick planar sheet with high strength and thermal conductivity [6]. But uniform dispersion of graphene in the matrix of aluminium alloys is the most challenging task. Few attempts have been made to proper dispersion of graphene in the matrix alloy.

Liu et al. [20] studied the characteristics of Al–graphene metal matrix composites through powder metallurgy method. The results show that the 0.15 wt.% of graphene reinforcement significantly improved the density and hardness of the composite. Bisht et al. [2] explored the mechanical behaviour of graphene sheets reinforced aluminium composites at different weight percentages through the spark plasma sintering. Mechanical properties are found to be high up to 1 wt.% graphene and thereafter the properties deteriorated due to agglomerated particles. Vignesh et al. [35] experimented with the graphene reinforced aluminium composites through powder metallurgy followed by hot extrusion. The outcome report indicates that the properties at high concentration of graphene improved through deformed grains as obtained by extrusion process. Subbaiah et al. [30] studied the characteristics of Al–graphene composites through stir casting process. The analysis confirmed that the mechanical properties noticeably decreased when graphene content exceeds 0.5

wt. %. These investigations confirmed that the properties in the aluminium composites are deteriorated with the addition of high concentrated graphene.

Al4032 alloy composites are used extensively in the fabrication of engine components, racing pistons and chassis components [17, 22]. Deepak et al. [7] investigated the properties of Al4032-SiC-GMP composites processed by stir-casting. Authors have noticed that decrements in mechanical properties were observed at 9 wt.% of reinforcement addition in Al4032 alloy. Rengasamy et al. [25] confirmed the mechanical properties of Al4032 alloy considerably increased with the addition of ZrB_2 and TiB_2 reinforcements.

A lot of research work carried out on aluminium alloy composites with the addition of different reinforcements by stir-casting. However, Al4032 composites are studied in a limited way. The accomplishment of strength as well as ductility in metal matrix composites (MMCs) is useful for a wide range of applications [15, 16].

Recently, severe plastic deformation (SPD) techniques have been applied to enhance the properties of metal matrix composites [8, 10]. Among all SPD processes, equal channel angular pressing (ECAP) is more attractive due to its cost effective, simple in operation and imparts significant strain in the material [21, 32]. Chidambaram et al. [5] investigated the mechanical properties of Al6061–5wt.%TiB_2 composite subjected to equal channel angular pressing (ECAP). The analysis revealed improvement in hardness, strength and elongation while following ECAP process. Rezaei et al. [26] analysed the effect of ECAP on the characteristics of aluminium matrix composites and confirmed that no reactive products formed at the interface of the matrix and reinforcement. Sun et al. [31] processed the Al-10SiCp composites through ECAP and identified the homogeneous equiaxed grains in the microstructure. The composite exhibited excellent strength and ductility after ECAP process. Lillo [19] enhanced the strength and ductility of Al-10B_4C composite through ECAP. Therefore, ECAP seems to be a better choice for the improvement of the properties in aluminium metal matrix composites (MMCs).

In the view of above literature, the property improvement of graphene reinforced aluminium composites via ECAP is not yet established. In this research work, Al4032 reinforced with graphene was fabricated by a stir casting process. The composites were extruded through ECAP after solution treatment up to 6 passes. The effects of ECAP and graphene addition on the microstructure and mechanical properties have been investigated.

Materials and Fabrication

The matrix material used in this research is Al4032 ingots which were supplied by Matrix Metal and Alloys, India. The Al4032 aluminium alloy reinforced with graphene sheet (10 μm, > 99.7%, Platelet) bought from Alfa Aesar, India. The alloy dispersed with four different concentrations (0%, 1%, 3% and 5%) wt.% of graphene by stir-casting method. Al4032 ingots were melted at 750 °C in a graphite crucible (Fig. 1a) and further the molten metal was degassed by using pure nitrogen. The graphene sheets were preheated up to 900 °C for 2 h in a separate muffle furnace. The particles are unified into the melt and stirred using a zircon-coated steel impeller about 10 min at 600 rpm to 1000 rpm. The composite melt was poured in preheated split-type permanent mould, and it was allowed to solidify normally.

The Al4032–graphene composites (Fig. 1b) were transformed into billets of 19.5 mm diameter and 110 mm length. The samples were annealed at 450 °C for 8 h and then cooled in the furnace. The homogenized samples were subjected to equal channel angular pressing (ECAP) through B_c route at 250 °C with a die having an intersection angle of 100°. Initially, the die was placed in a furnace (Fig. 1c) and heated up to 250 °C, and also the billets were preheated to the required temperature in a muffle furnace. Once the required die temperature attains, the billet is placed in a die and extruded immediately using a hydraulic press with a ram speed of 1 mm/sec. The die temperature was controlled by thermocouple and monitored continuously during the process. MoS_2 was used as a lubricant during the ECAP process. The composite specimens were pressed up to 6 passes and the sample characterization was done at each pass. Figure 1d shows the Al4032–graphene specimens after ECAP.

The samples for microstructural study were ground with standard SiC abrasive papers up to 1000 grit size and subsequently polished with Al_2O_3 paste on a velvet cloth. The surface morphology was studied using a metallurgical microscope (Chennai Metco, India) and scanning electron microscope (Hitachi S300N, Japan) equipped with energy dispersive spectroscopy (EDS). The hardness test results for Al4032–graphene composites were measured using Vickers hardness tester (MATSUZAWA, MMT-X7). A load of 1 kg is applied for a dwell time of 15 s, and the average hardness was taken at five measurement points. The tensile test of composites was conducted at room temperature as per ASTM-E8 standard. The test was carried out on an Instron mechanical testing machine with load cell capacity of 50 KN and strain rate of 1 mm/min.

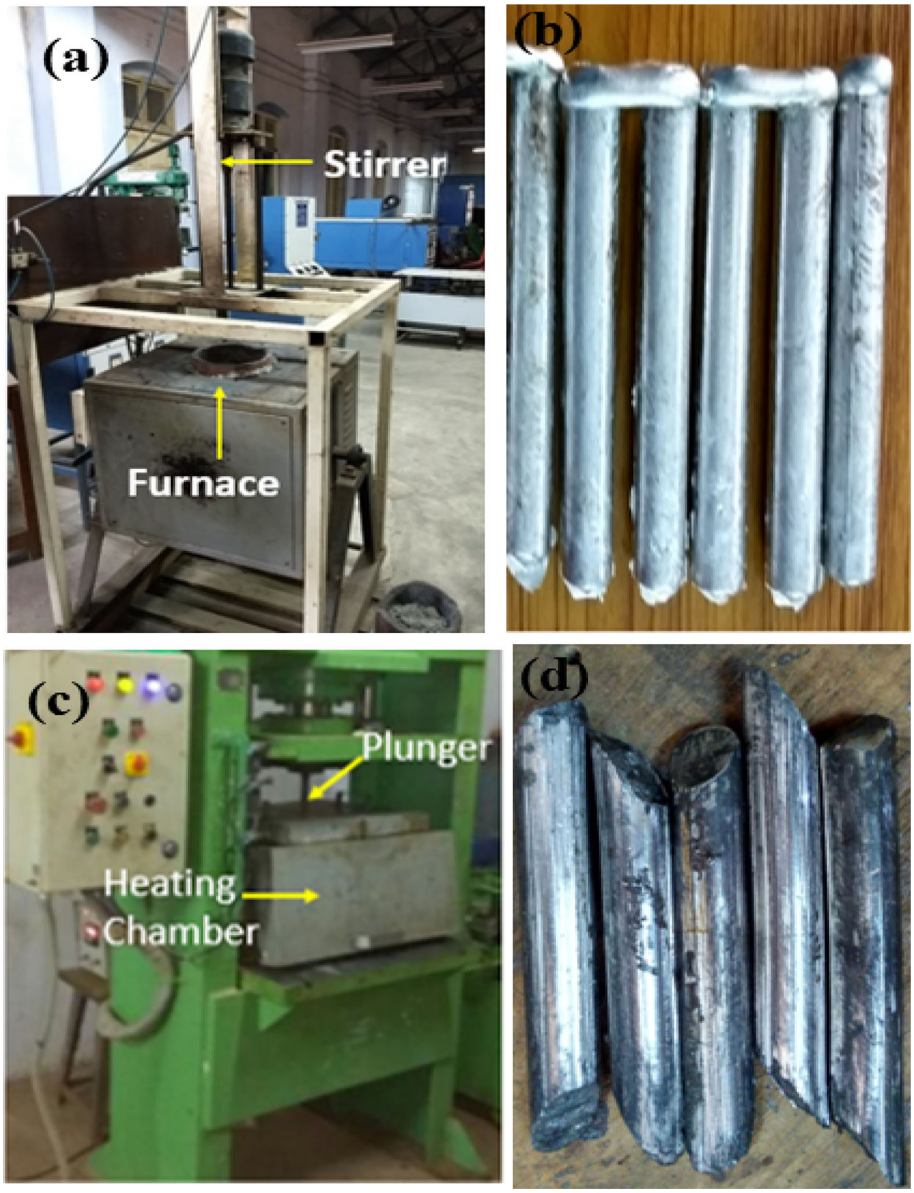

Fig. 1 Al4032–graphene composites: Stir-casting **(a)** furnace and **(b)** samples; **(c)** ECAP setup; **(d)** ECAPed samples

Results and Discussions

Microstructure

Table 1 shows the chemical composition of different specimens of Al4032–graphene metal matrix composites. The optical microstructure (OM) of Al4032–1%graphene composite is shown in Fig. 2. In the as-cast composite (Fig. 2a), the coarse grained structure is observed. After annealing (Fig. 2b), the grains are refined, and the complete homogenized structure is perceived. The grains are further refined with 1 pass ECAP process as shown in Fig. 2c. The specimen processed by 6 pass ECAP (Fig. 2d) showed broken grain boundary flow along the extrusion direction.

Table 1 Composition of Al4032–graphene composites

S. No	Specimen	Al4032 (Wt.%)	Graphene (Wt.%)
1	Al4032	100	0
2	Al4032–1%graphene	99	1
3	Al4032–3%graphene	97	3
4	Al4032–5%graphene	95	5

The SEM image of Al4032–3%graphene composite at homogenized condition is shown in Fig. 3a. The EDS

analysis in Fig. 3b confirmed the existence of graphene particles in alloy matrix. One can observe that some of the graphene particles are precipitated at the grain boundaries. Figure 3c and d shows the even distribution of grains and graphene particles with ECAP process. The specimen processed by 2 pass ECAP (Fig. 3c) shows refined grains with graphene particles along the pressing direction. The microstructure of Al4032 composite has been changed after 6 pass ECAP and significant refinement in grain size has been observed.

The variation in grain size of Al4032–graphene composites with ECAP process is given in Table 2. As seen, there is a large deviation in the grain size of composites before and after the ECAP process. The average grain size of 3% graphene reinforced specimen at homogenized condition is 46.63 μm. The grains are refined and reduced to 36.52 μm (Fig. 3d) with 2-pass ECAP. The grains are further refined and reduced to 15.01 μm (Fig. 3f) with the continuation of an ECAP process up to 6 passes. From Table 2, it is also noted that the average grain size of Al4032–graphene composites increased when the graphene content exceeds 1 wt.%.

In order to better understand the graphene dispersion in the Al4032 matrix, an SEM image at high magnification is given in Fig. 4. The composite (Al4032–3%graphene) processed at homogenized condition shows agglomerated graphene particles (Fig. 4a) at the grain boundaries. After 6 passes of ECAP, the precipitation of dispersed graphene particles is formed at the grain boundaries (Fig. 4b). Overall, the Al4032 composite microstructure is refined by breaking down the grain size and homogeneous dispersion of graphene particles with the increase in the number of passes. Al4032–5%graphene (Fig. 4c and d) showed similar changing trends in microstructure at all conditions. However, the agglomerated particles in Al4032 matrix are more with the dispersion of 5% of graphene (Fig. 4c) compared to the 3% of graphene (Fig. 4a).

Mechanical Properties

Hardness

The variation in the hardness of graphene-dispersed Al4032 composites at different conditions is shown in Fig. 5, and the values are listed in Table 3. The hardness of Al4032 alloy at homogenized condition was 54.13 HV. The hardness increased by 5.4% with the addition of 1% graphene (Fig. 5b) and 5.05% with the addition of 3% graphene (Fig. 5c) at the same condition. One can note that the hardness decreased by 0.1% with the addition of 5% graphene (Fig. 5d). This may be due to uneven dispersion of graphene particles and more agglomerated particles as observed in the microstructure of Al4032–5%graphene composite (Fig. 4c).

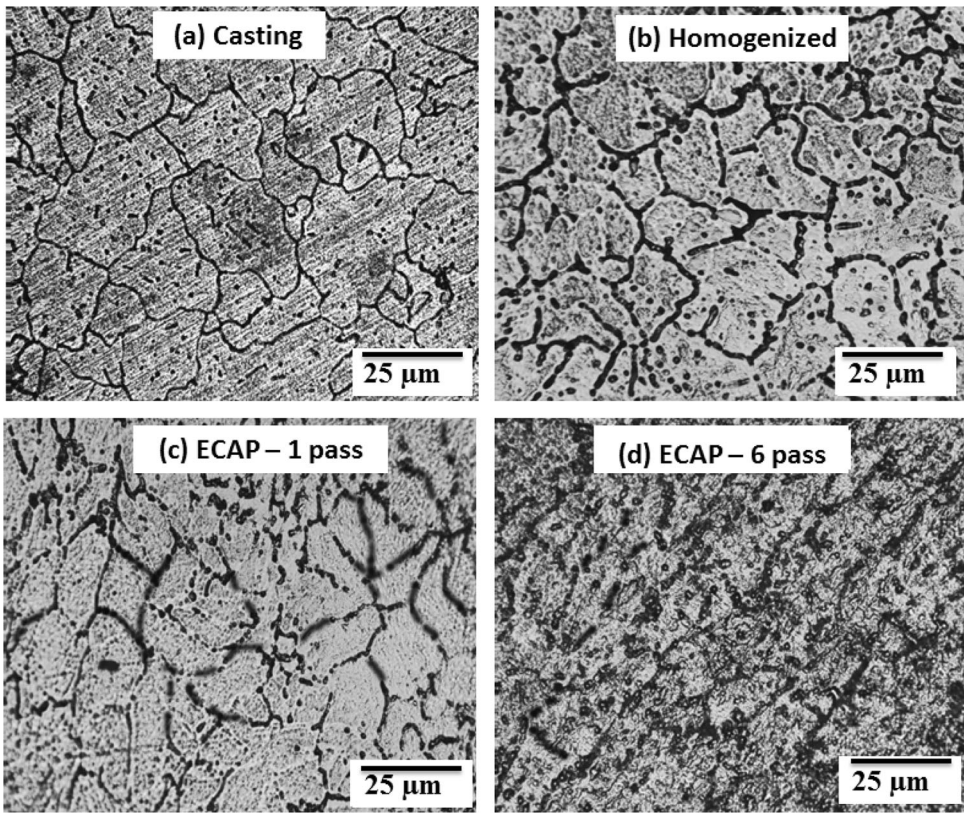

Fig. 2 Optical microstructure of Al4032–1%graphene: **(a)** as cast alloy; **(b)** as homogenized alloy; **(c)** 1-pass ECAP; (d) 6-pass ECAP

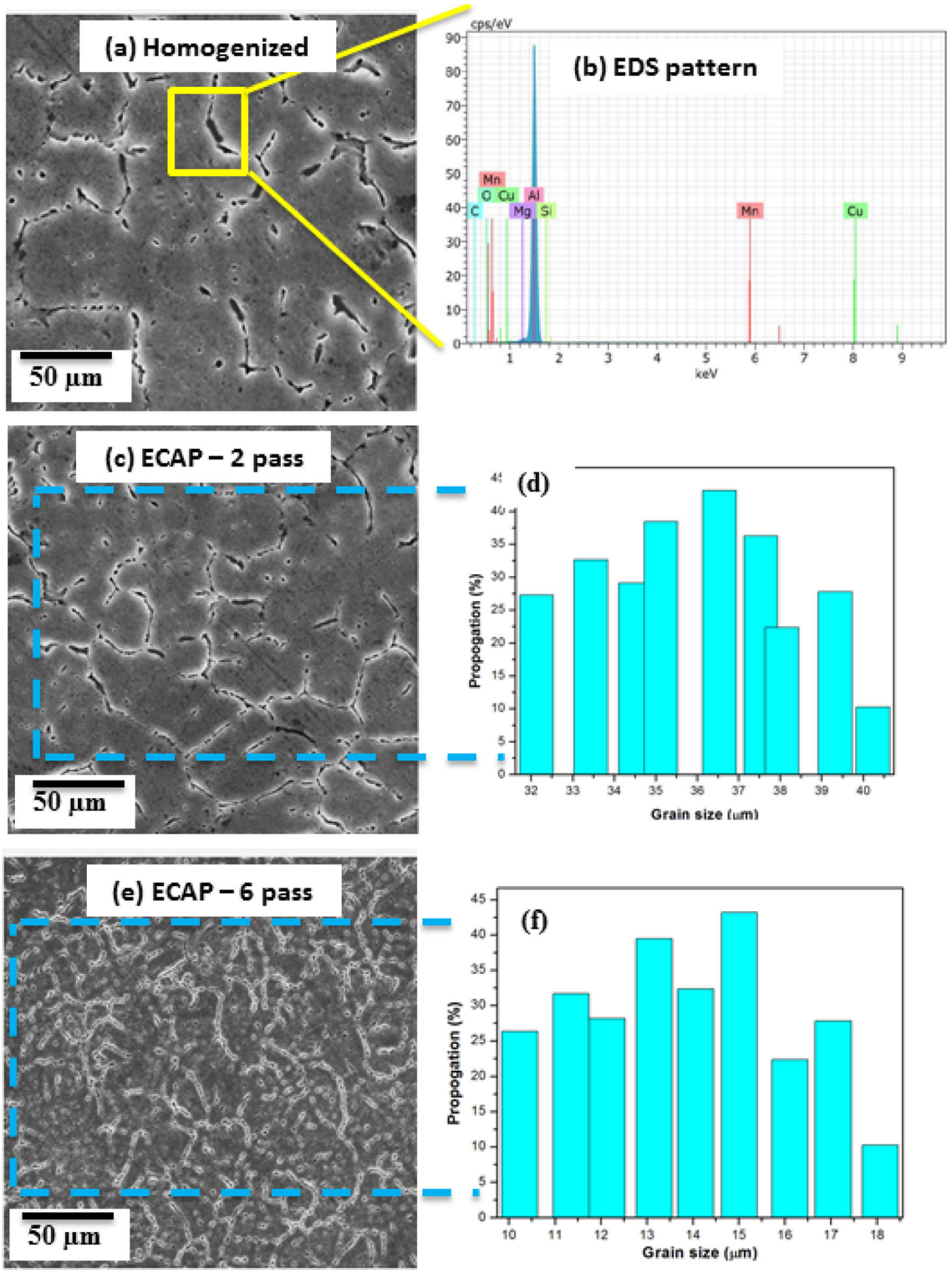

Fig. 3 SEM images of Al4032–3%graphene composite: **(a)** and **(b)** Homogenized alloy; **(c)** and **(d)** 2-pass ECAP; **(e)** and **(f)** 6-pass ECAP

The Al4032 alloy reinforced with 3% of graphene showed a hardness of 57.01 HV at homogenized condition. The hardness increases with 1-pass ECAP by 9.8%. After 2-pass ECAP, the increase in hardness of Al4032–3%-graphene composite is about 19%. On further continuation of ECAP passes to 6, the hardness values grow and

Table 2 Average grain size of Al4032–graphene composites

Sample	Homogenized Grain size (μm)	ECAP-1 pass Grain size (μm)	ECAP-2 pass Grain size (μm)	ECAP-3 pass Grain size (μm)	ECAP-4 pass Grain size (μm)	ECAP-5 pass Grain size (μm)	ECAP- 6 pass Grain size (μm)
Al4032	62.21	60.32	52.19	44.43	36.35	31.61	29.31
Al4032–1%graphene	45.11	43.35	35.23	30.42	21.41	15.42	14.33
Al4032–3%graphene	46.63	44.31	36.52	31.65	22.32	16.65	15.01
Al4032–5%graphene	50.21	48.34	40.54	35.63	26.63	20.52	19.19

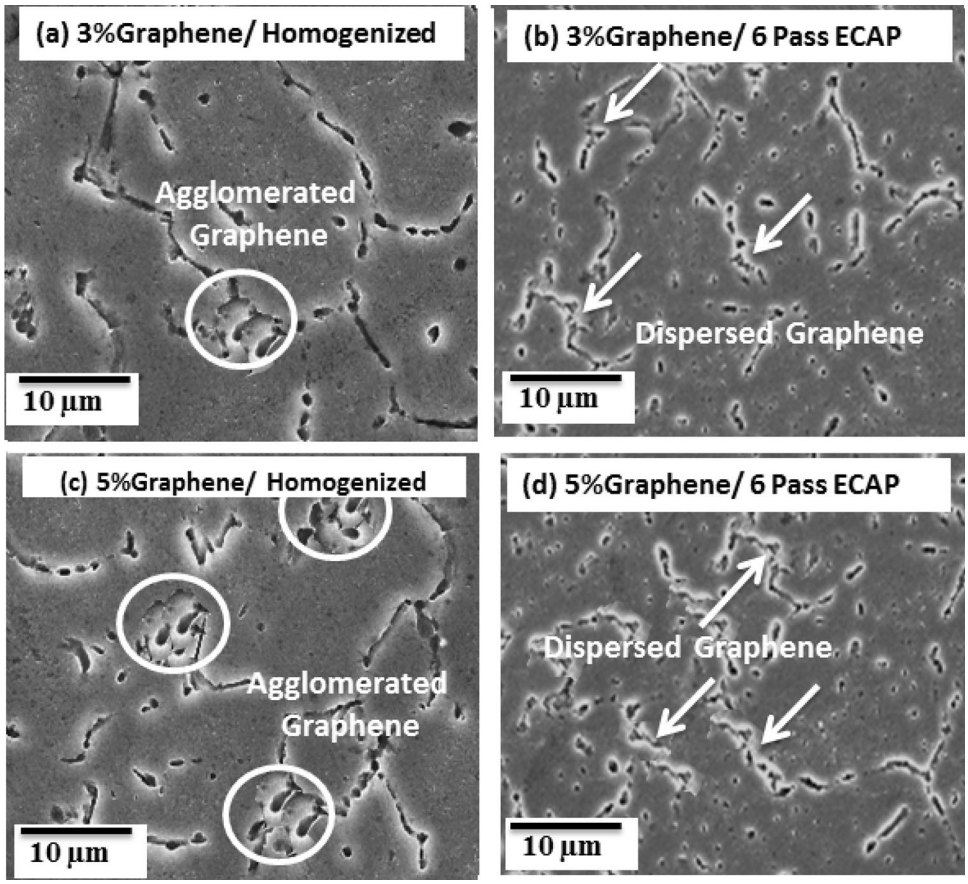

Fig. 4 Microstructure of composites: **(a)** and **(b)** Al4032–3%graphene composites; **(c)** and **(d)** Al4032–5%graphene composites

increased by 28%. The refined grain structure, number of deformed grains and even dispersion of graphene particles are the reasons for improvement in hardness after 6-pass ECAP.

Tensile Properties

Figure 6 shows the typical engineering stress–strain curves for Al4032–graphene composites at different processing methods. The tensile properties (strength and ductility) are shown in Figs. 7 and 8. The addition of 1% graphene causes the maximum tensile strength in Al4032 alloy (Table 4). The further addition of graphene (3% and 5%) leads to a decrease in UTS. The decrease in UTS for homogenized Al4032–5% graphene was 4% when compared to homogenized Al4032–1% graphene. The possible reason for this effect is that graphene sheets are not properly aligned in the matrix alloy (Fig. 4c). The precipitation of agglomerated particles may create cavities, and also weakens the reinforcement/Al matrix interface [29]. These are the reasons for decrement in tensile strength of Al4032–5% graphene composite at homogenized condition.

As shown in Fig. 8, the elongation in homogenized Al4032 alloy decreases with the addition of graphene sheets. The elongation for matrix alloy in homogenized condition is 8.13%. This value is respectively decreased to 6.98%, 4.75% and 2.81% after 1%, 3% and 5% dispersion

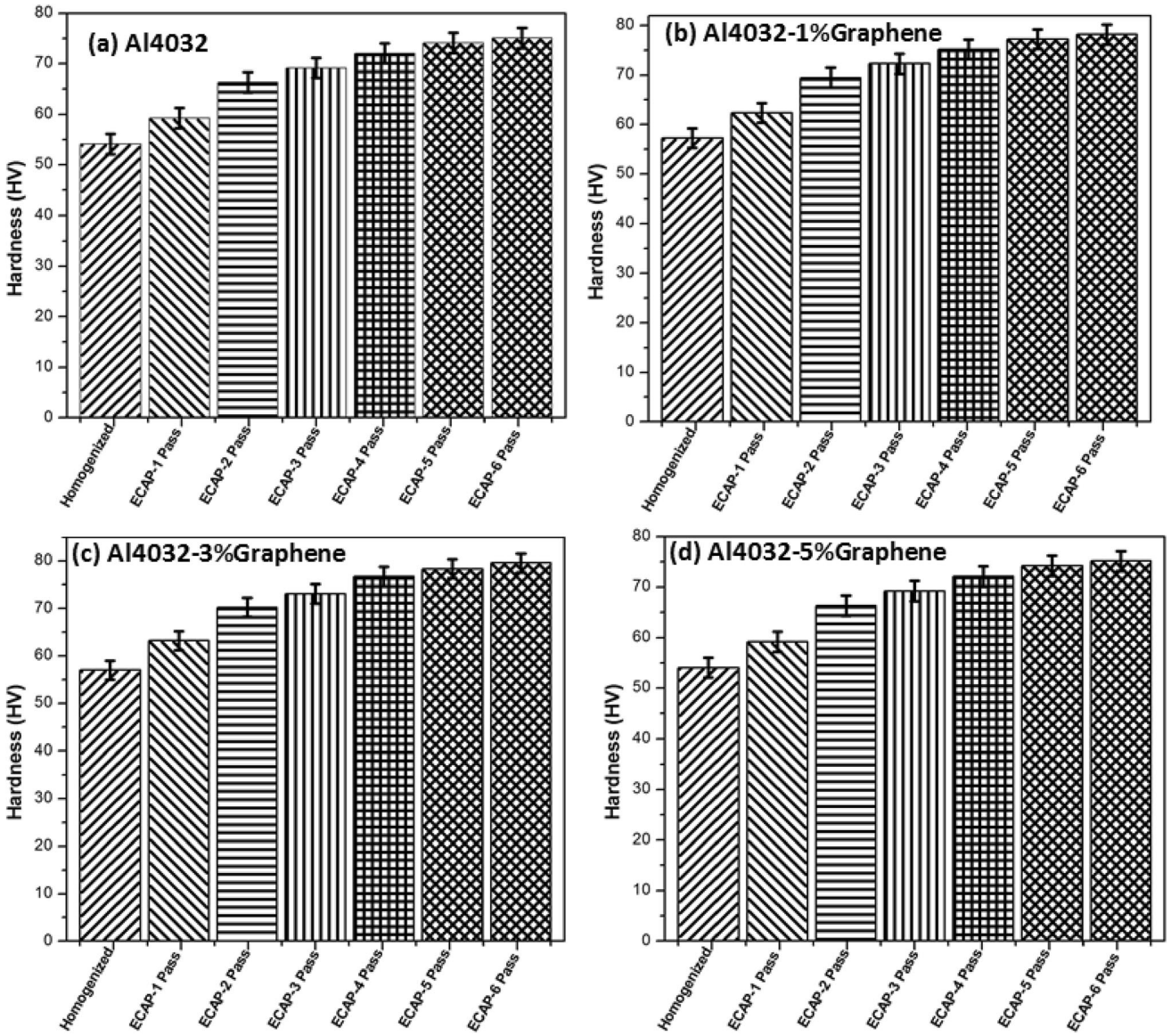

Fig. 5 Hardness variation of Al4032–graphene composites

Table 3 Hardness of Al4032–graphene composites

Sample	Homogenized Hardness (HV)	ECAP-1 pass Hardness (HV)	ECAP-2 pass Hardness (HV)	ECAP- 3 pass Hardness (HV)	ECAP- 4 pass Hardness (HV)	ECAP- 5 pass Hardness (HV)	ECAP- 6 pass Hardness (HV)
Al4032	54.13	59.24	66.32	69.16	72.06	74.11	75.06
Al4032–1%graphene	57.25	62.36	69.44	72.28	75.18	77.23	78.18
Al4032–3%graphene	57.01	63.21	70.24	73.08	76.71	78.31	79.54
Al4032–5%graphene	54.06	59.18	66.34	69.21	72.11	74.21	75.12

of graphene in the matrix alloy. The precipitation of hard graphene sheets in aluminium matrix alloy improves the brittle nature of the composite [24].

From Fig. 6a–d, the tensile properties of Al4032 composites are improved by ECAP process. The 1-pass Al4032–1% graphene MMC showed UTS of 168.48 MPa (Table 4). After 2-pass ECAP, the UTS of composite

further increased to 180.52 MPa. A similar trend has been observed for further continuation of an ECAP process up to 6 passes. The UTS and elongation are increased by 33% and 5% after 6-pass ECAP as compared to homogenized condition. This is due to the combined effect of reinforcement (graphene) addition and severely deformed grains.

Fractographic studies

The surface morphology of Al4032–graphene composites after tensile test is shown in Fig. 9. The SEM image (Fig. 9a and c) of as-homogenized composite shows a brittle fracture with coarse grain structure and pores also observed. However, the fracture surface morphology of 5% graphene added composite (Fig. 9c) shows large pores with re-arranged particles. It is clear that the fracture occurs at homogenized condition is due to void nucleation and thus creates the stress concentration at the matrix–particle interface [14]. These observations are coincident with the poor mechanical properties of homogenized Al4032–graphene composites (Fig. 6).

The fracture morphology (Fig. 9b and d) of ECAPed composite shows relatively smooth fractured surface and faceted. The pores or cavities have been eliminated by continuing ECAP up to 6 passes. It is to be noted that the ECAPed composite indicates the brittle failure with the flat fracture surface. As shown in Fig. 8b and d, the graphene surface is quite rough and pits also observed, which specifies that the strong interface bonding between matrix and reinforced particles [9]. These observations illustrate that the ECAP method enhances the mechanical properties (Table 4) and improve the microstructure of Al4032–graphene composites (Fig. 3).

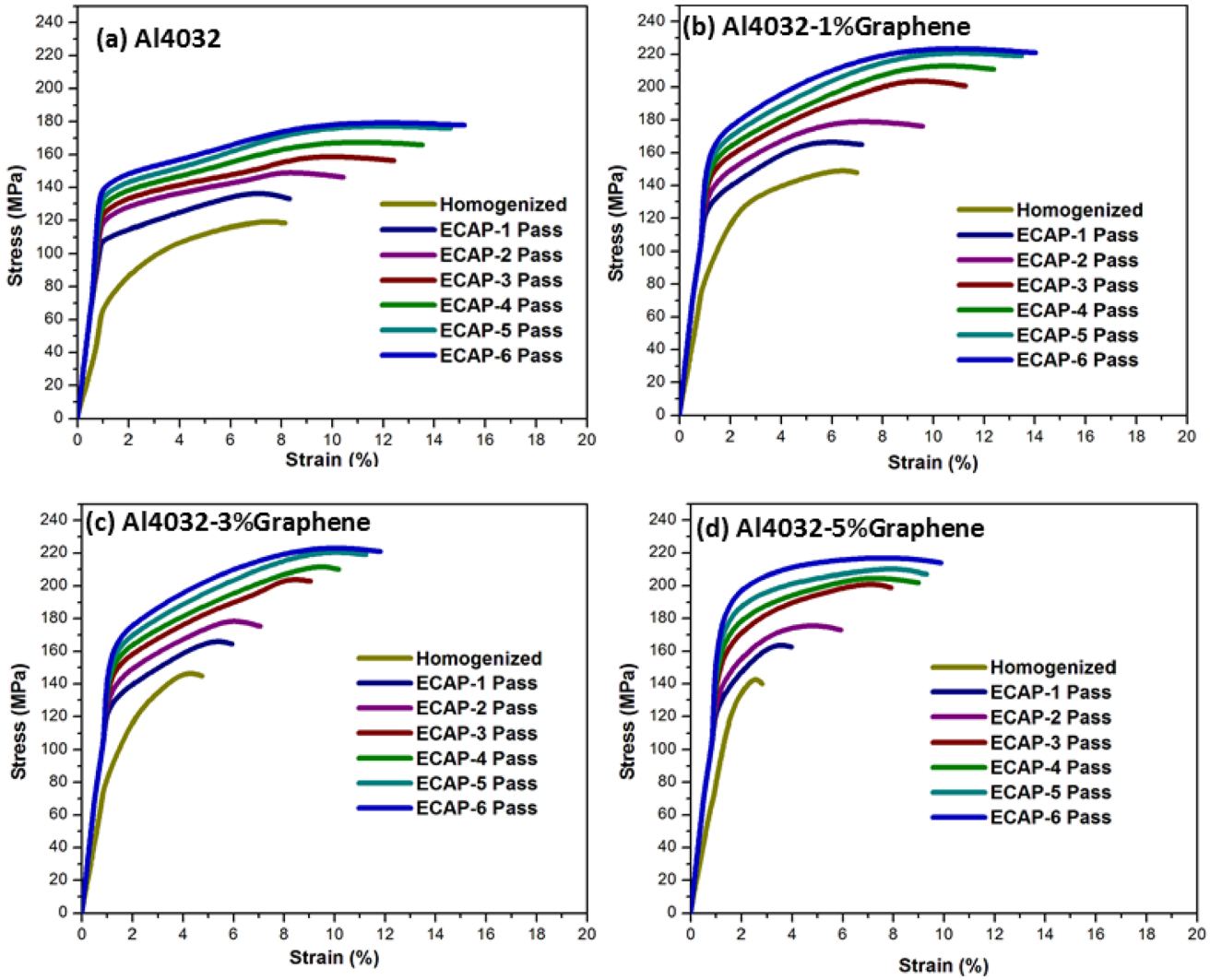

Fig. 6 Engineering stress–strain curves for Al4032–graphene composites

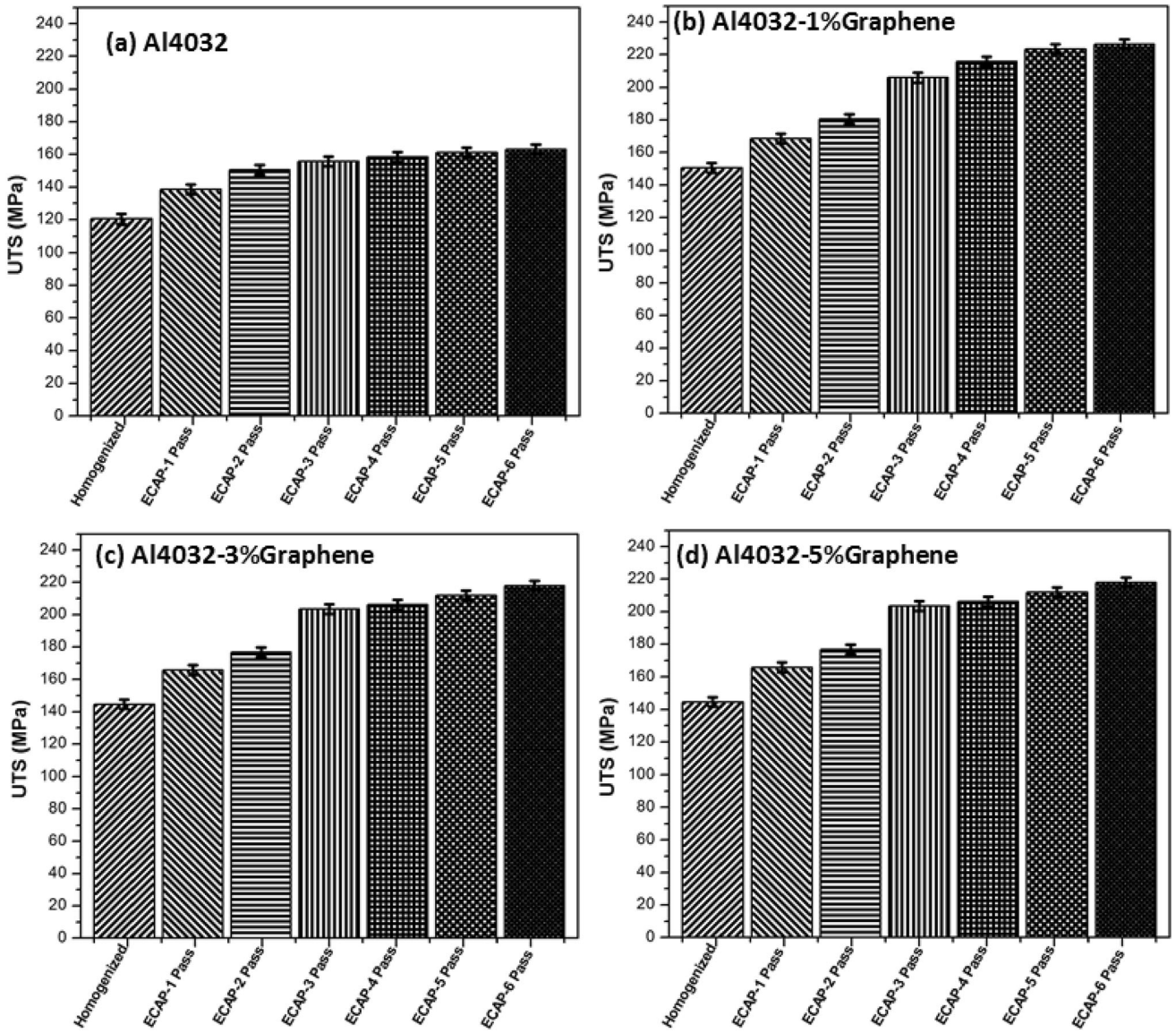

Fig. 7 Tensile strength values for Al4032–graphene composites

Discussion on Dispersion of High-content Graphene with ECAP

The development of Al4032–graphene composites was studied as a function of the weight fraction of the graphene with ECAP process. The addition of graphene in base matrix leads to morphology transition. The ECAP process has positively influenced the microstructure and causes the reduced dendritic structure (Fig. 2). A maximum of six passes was done with 100° ECAP die. When increasing the number of ECAP passes, the grain refinement was present in all compositions of the Al4032–graphene composites. The microstructure of ECAPed samples revealed more number of sub grains along with elongated grain structure (Fig. 3c and e).

The addition of different weight fractions of graphene has no significant effect on the grain size of Al4032 composite. The increase in graphene content (≥ 3 wt.%) leads to formation of agglomeration (Fig. 4a and c) during fabrication rather than dispersing into matrix alloy [36]. This may be the reason for the increase in the average grain size at 3 and 5wt.% graphene composition (Table 2). The ECAP has a significant effect on the microstructure of higher content (≥ 3 wt.%) graphene compositions. The grain size is refined by breaking down the grain with the increase in the number of passes in ECAP. The microstructure of the Al4032–5% graphene sample was refined from an unprocessed sample of grain size 50.21 to 19.19 μm after 6 passes (Table 2). And also, the

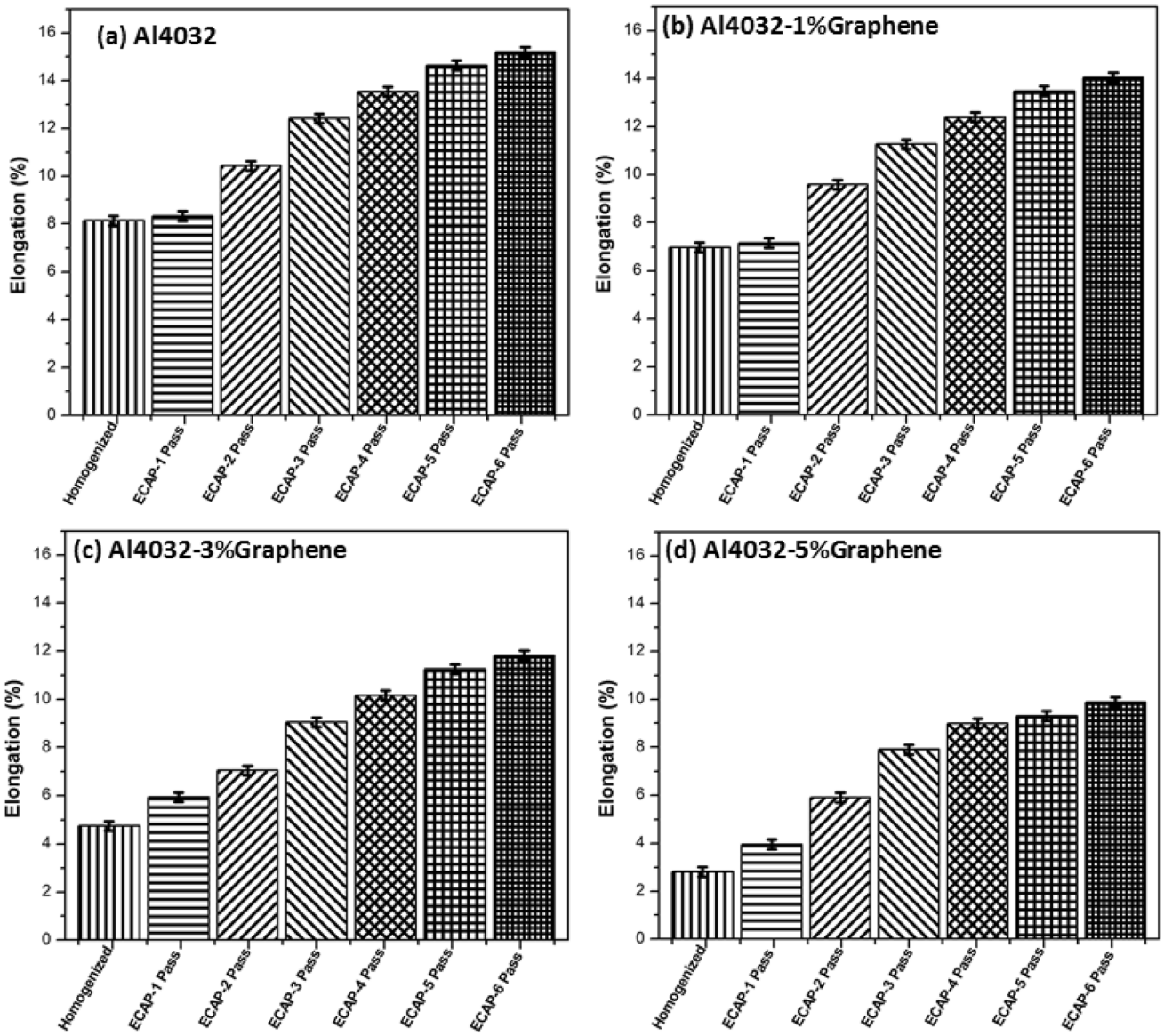

Fig. 8 Elongation values for Al4032–graphene composites

agglomerated graphene was decomposed to distributed particles after 6-pass ECAP (Fig. 4).

The 6-pass ECAPed samples proved beneficial in refined microstructure with a deformed grain distribution that has resulted in improved mechanical properties. The abrupt improvement in the mechanical properties has been observed after severe deformation at higher content graphene compositions. The hardness of homogenized Al4032–5%graphene is increased from 54.06 HV to 75.12 HV after 6-pass ECAP. The improved microstructure with dispersed graphene particles as obtained due to the assistance of ECAP is a dominant factor in achieving the hardness improvement [27].

The 5 wt.% of the graphene composite with ECAP showed an improvement in UTS of 27% as compared to the as homogenized matrix alloy. This improvement may be due to the homogeneous dispersion of graphene particles (Fig. 4d) caused by ECAP, which impede movement of dislocation and thereby promotes strengthening [28]. The graphene particle acts as nucleation during deformation and leads to grain refinement, which causes strength improvement [18].

The mechanical properties of investigating compositions are compared with the Al–graphene compositions developed by others (Table 5). The Al4032 alloy of 1%, 3% and 5% graphene compositions fabricated through stir casting and homogenization followed by ECAP attained comparable values.

Table 4 Tensile properties of Al4032–graphene composites

Sample	Homogenized UTS (MPa)	ECAP- 1 pass UTS (MPa)	ECAP- 2 pass UTS (MPa)	ECAP- 3 pass UTS (MPa)	ECAP- 4 pass UTS (MPa)	ECAP- 5 pass UTS (MPa)	ECAP- 6 pass UTS (MPa)
Al4032	120.32	138.35	150.39	155.64	158.55	161.25	163.17
Al4032–1%graphene	150.45	168.48	180.52	205.85	215.76	223.46	226.38
Al4032–3%graphene	148.01	167.83	179.87	205.02	214.01	222.91	225.73
Al4032–5%graphene	144.64	165.73	176.66	203.43	206.34	212.04	217.96
Sample	Homogenized PE (%)	ECAP- 1 pass PE (%)	ECAP- 2 pass PE (%)	ECAP- 3 pass PE (%)	ECAP- 4 pass PE (%)	ECAP- 5 pass PE (%)	ECAP- 6 pass PE (%)
Al4032	8.13	8.32	10.43	12.42	13.54	14.63	15.19
Al4032–1%graphene	6.98	7.17	9.58	11.27	12.39	13.48	14.04
Al4032–3%graphene	4.75	5.94	7.05	9.04	10.16	11.25	11.81
Al4032–5%graphene	2.81	3.96	5.91	7.91	8.99	9.31	9.88

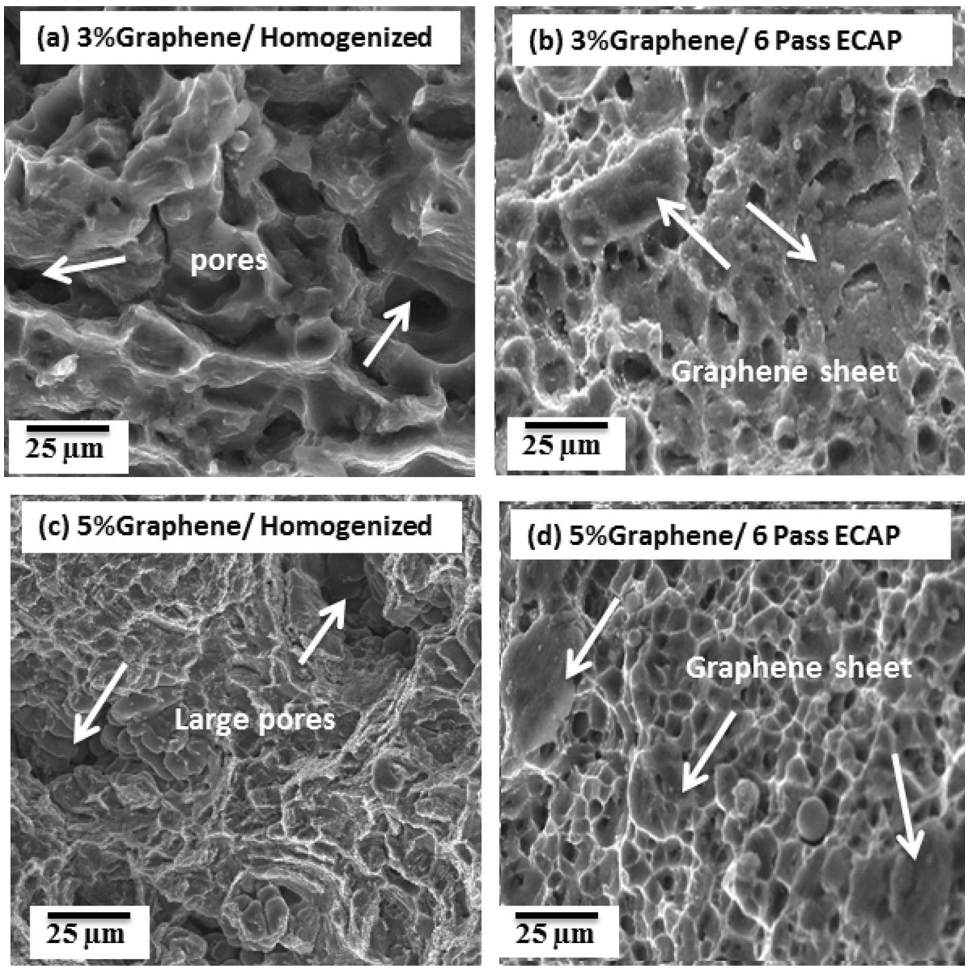

Fig. 9 Fracture surface morphology of Al4032–graphene composites

Table 5 Mechanical properties comparison between Al–graphene composites and corresponding matrix alloy developed by different processing routes

Fabrication method	Composition	Hardness variation (%)	Strength variation (%)	Remarks (Compared to the corresponding highest value)	Reference
Powder metallurgy	Al6061–0.5 graphene	+ 27.4%	+ 27.4%	–	[13]
	Al6061–1 graphene	+ 33.8%	+ 32%	–	
	Al6061–3 graphene	+ 10%	+ 12%	Hardness decreased by 23.8% Strength decreased by 20%	
MA + ECAP	Al6061-0.25 graphene	+ 37.2%	+ 53.7%	–	[1]
	Al6061–0.5 graphene	+ 33.6%	+ 51%	Hardness decreased by 3.6% Strength decreased by 2.7%	
	Al6061–1 graphene	+ 23.5%	+ 42.5%	Hardness decreased by 13.7% Strength decreased by 11.2%	
Stir casting + Homogenization	Al–0.5 graphene	+ 55.3%	+ 12.7%	–	[30]
	Al–1 graphene	+ 42.6%	+ 10%	Hardness decreased by 12.7% Strength decreased by 2.7%	
	Al–2 graphene	+ 28%	− 15.5%	Hardness decreased by 27.3% Strength decreased by 28.2%	
MA + Hot pressing	AA2219–0.5 graphene	− 0.1%	–	Hardness decreased	[23]
	AA2219–1 graphene	− 0.3%	–		
	AA2219–2 graphene	− 0.5%	–		
Friction stir processing	Al5052– graphene	–	− 12%	Strength decreased by 12%	[12]
Ultrasonic assisted stir casting process	AA7075–0.3 graphene	+ 6%	+ 16%	–	[4]
	AA7075–0.5 graphene	+ 12%	+ 13%	Strength decreased by 3%	
Stir casting + Homogenization + ECAP	Al4032–1%graphene	+ 30%	+ 47%	–	Present work
	Al4032–3%graphene	+ 32%	+ 46.9%	Strength decreased by 0.1%	
	Al4032–5%graphene	+ 28%	+ 44%	Hardness decreased by 4% Strength decreased by 2%	

Conclusions

In the present work, the Al4032–graphene composites were fabricated through stir casting followed by solution treatment. The homogenized composites were subjected to 6-pass ECAP with 100° ECAP die. The influence of 6-pass ECAP on microstructure and mechanical properties were studied, and the conclusions of this work could be drawn as follows:

1. The ECAP process effectively refined the grain structure of the graphene/Al4032 with intense graphene precipitation.
2. Highest hardness value for the fabricated composites was recorded for 3% graphene with 6-pass ECAP condition.
3. The tensile properties of graphene/ Al4032 composites were effectively improved after 6-pass ECAP. The UTS of ECAPed composite were approximately 1.5 times higher than the homogenized composite.
4. The elongation of graphene/ Al4032 composites decreases with the increase in graphene content and increases with the increase in ECAP passes.
5. The fracture surface of graphene/Al4032 composites after ECAP was a mixed mode of failure. The Al4032–graphene interface bonding was good at higher passes of ECAP.

Based on the above conclusions, the homogenized graphene compositions in Al4032 matrix facilitate better mechanical properties through ECAP process.

Acknowledgements The authors would like to thank Anna University College of Engineering, Chennai, India, for providing ECAP and mechanical testing facilities. The SEM analysis in the present investigation was carried out at the Indian Institute of Technology Madras (IITM), India.

Funding Funding is not applicable to this work.

Declarations

Conflict of interest Authors declare that there is no conflict of interest.

References

1. H. Azar, B. Sadri, A. Nemati et al., Investigating the microstructure and mechanical properties of aluminum-matrix reinforced-graphene nanosheet composites fabricated by mechanical milling and equal-channel angular pressing. Nanomaterials **9**, 1070 (2019). https://doi.org/10.3390/nano9081070
2. A. Bisht, M. Srivastava, R. Manoj, I. Lahiri, D. Lahiri, Strengthening mechanism in graphene nanoplatelets reinforced aluminum composite fabricated through spark plasma sintering. Mater. Sci. Eng., A **695**, 20–28 (2017). https://doi.org/10.1016/j.msea.2017.04.009
3. M. Bodunrin, K. Alaneme, L. Chown, Aluminium matrix hybrid composites: a review of reinforcement philosophies; mechanical, corrosion and tribological characteristics. J. Market. Res. **4**, 434–445 (2015). https://doi.org/10.1016/j.jmrt.2015.05.003
4. V. Chak, H. Chattopadhyay, Fabrication and heat treatment of graphene nanoplatelets reinforced aluminium nanocomposites. Mater. Sci. Eng., A **791**, 139657 (2020). https://doi.org/10.1016/j.msea.2020.139657
5. A. Chidambaram, S.B. Prabu, K.A. Padmanabhan, Microstructure and mechanical properties of AA6061–5wt.%TiB2 in-situ metal matrix composite subjected to equal channel angular pressing. Mater. Sci. Eng., A **759**, 762–769 (2019). https://doi.org/10.1016/j.msea.2019.05.068
6. S. Das, S. Khanna, D.P. Mondal, Graphene-reinforced aluminum hybrid foam: response to high strain rate deformation. J. of Materi Eng and Perform **28**, 526–534 (2019). https://doi.org/10.1007/s11665-018-3815-7
7. K. Deepak. et al. (2021). Morphological and mechanical characterization of Al-4032/SiC/GMP hybrid composites. https://www.researchsquare.com/article/rs-232039/v1
8. R. Derakhshandeh-Haghighi, S.A. JenabaliJahromi, The effect of multi-pass equal-channel angular pressing (ecap) for consolidation of aluminum-nano alumina composite powder on wear resistance. J. of Mater Eng Perform **25**, 687–696 (2016). https://doi.org/10.1007/s11665-016-1888-8
9. E. Ghasali, P. Sangpour, A. Jam et al., Microwave and spark plasma sintering of carbon nanotube and graphene reinforced aluminum matrix composite. Archiv. Civ. Mech. Eng **18**, 1042–1054 (2018). https://doi.org/10.1016/j.acme.2018.02.006
10. Z. Horita, K. Oh-ishi, K. Kaneko, Microstructure control using severe plastic deformation. Sci. Technol. Adv. Mater. **7**, 649–654 (2006). https://doi.org/10.1016/j.stam.2006.05.011
11. D. Hülya, G. Canser, Ç. Nilay, Y. Melis, An investigation into the wear behavior of aged Alumix321/SiC composites fabricated by hot pressing. Rev. Metal. **55**(3), e148 (2019). https://doi.org/10.3989/revmetalm.148
12. C. Jeon, Y. Jeong, J. Seo et al., Material properties of graphene/aluminum metal matrix composites fabricated by friction stir processing. Int. J. Precis. Eng. Manuf **15**, 1235–1239 (2014). https://doi.org/10.1007/s12541-014-0462-2
13. Md. Khan, R.U. Din, A. Wadood et al., Effect of graphene nanoplatelets on the physical and mechanical properties of Al6061 in fabricated and T6 thermal conditions. J. Alloy. Compd. **790**, 1076–1091 (2019). https://doi.org/10.1016/j.jallcom.2019.03.222
14. P.K. Kumar et al., Effect of compaction pressure on mechanical properties of powder steel 0.06% C – 22% Cr – 13% Ni – 5% Mn – 2% Mo obtained by mechanical alloying followed by annealing. Met Sci Heat Treat **63**, 132–139 (2021). https://doi.org/10.1007/s11041-021-00659-9
15. P.K. Kumar, N.V. Sai, A.G. Krishna, Influence of sintering conditions on microstructure and mechanical properties of alloy 218 steels by powder metallurgy route. Arab. J. Sci. Eng. **10**, 116–121 (2018). https://doi.org/10.1007/s13369-017-3015-z
16. K. Kumar et al., Effect of Y_2O_3 addition and cooling rate on mechanical properties of Fe-24Cr-20Ni-2Mn steels by powder metallurgy route. Compos. commun **10**, 116–121 (2018). https://doi.org/10.1016/j.coco.2018.09.003
17. D. Kumar, K.S. Pradeep, Microstructural and mechanical characterization of Al-4032 based metal matrix composites. Mater Today: Proc **18**, 2563–2572 (2019). https://doi.org/10.1016/j.matpr.2019.07.114
18. F.H. Latief, El. Sayed, M. Sherif, Effects of sintering temperature and graphite addition on the mechanical properties of aluminum. J. Ind. Eng. Chem. **18**, 2129–2134 (2012). https://doi.org/10.1016/j.jiec.2012.06.007
19. T.M. Lillo, Enhancing ductility of AL6061+10wt.% B4C through equal-channel angular extrusion processing. Mater. Sci. Eng., A **410**, 443–446 (2005). https://doi.org/10.1016/j.msea.2005.08.093
20. J. Liu, U. Khan et al., Graphene oxide and graphene nanosheet reinforced aluminium matrix composites: powder synthesis and prepared composite characteristics. Mater. Des. **94**, 87–94 (2016). https://doi.org/10.1016/j.matdes.2016.01.031
21. G.K. Manjunath, G.V. Preetham Kumar, K. Udaya Bhat et al., Microstructure and mechanical properties of cast Al-5Zn-2Mg alloy subjected to equal-channel angular pressing. J Mater Eng and Perform **27**, 5644–5655 (2018). https://doi.org/10.1007/s11665-018-3691-1
22. L.F. Mondolfo, Aluminium Alloys, Butterworths & Co Ltd, Elsevier. https://www.elsevier.com/books/aluminum-alloys/mondolfo/978-0-408-70932-3 (1976)
23. L.K. Pillari et al., Processing and characterization of graphene and multi-wall carbon nanotube-reinforced aluminium alloy AA2219 composites processed by ball milling and vacuum hot pressing. Metallogr. Microstruct. Anal. **6**, 289–303 (2017). https://doi.org/10.1007/s13632-017-0365-6
24. R. Raj, J.M.S. YoganandhSaravanan et al., Effect of graphene addition on the mechanical characteristics of AA7075 aluminium nanocomposites. Carbon Lett (2020). https://doi.org/10.1007/s42823-020-00157-7
25. N.V. Rengasamy et al., An analysis of mechanical properties and optimization of edm process parameters of Al 4032 alloy reinforced with Zrb_2 and Tib_2 In-Situ composites. J. Alloy. Compd. **662**, 325–338 (2016). https://doi.org/10.1016/j.jallcom.2015.12.023
26. M.R. Rezaei, S.G. Shabestari, S.H. Razavi, Effect of ECAP consolidation process on the interfacial characteristics of Al-Cu-Ti metallic glass reinforced aluminum matrix composite. Compos. Interfaces **25**, 669–679 (2018). https://doi.org/10.1080/09276440.2018.1439619
27. M. Saravanan, R.M. Pillai, K.R. Ravi, B.C. Pai, M. Brahmakumar, Development of ultrafine grain aluminium–graphite metal matrix composite by equal channel angular pressing. Compos.

Sci. Technol. **67**, 1275–1279 (2007). https://doi.org/10.1016/j.compscitech.2006.10.003
28. S.E. Shin, D.H. Bae, Deformation behavior of aluminum alloy matrix composites reinforced with few-layer graphene. Compos. A Appl. Sci. Manuf. **78**, 42–47 (2015). https://doi.org/10.1016/j.compositesa.2015.08.001
29. S. Soltani, R.R.T. KhosroshahiMousavian et al., Stir casting process for manufacture of Al–SiC composites. Rare Met. **36**, 581–590 (2017). https://doi.org/10.1007/s12598-015-0565-7
30. V. Subbaiah, B. Palampalle, K. Brahmaraju, Microstructural analysis and mechanical properties of pure Al–GNPs composites by stir casting method. J. Inst. Eng. India Ser. C **100**, 493–500 (2019). https://doi.org/10.1007/s40032-018-0491-1
31. Y.P. Sun, J. Han, Y. Tu, Z. Bai, Y.Q. He, Microstructure and mechanical properties of a spray deposited SiCp/Al composite processed by hot extrusion and equal channel angular pressing. Mater. Res. Innovations **18**, 220–223 (2014). https://doi.org/10.1179/1432891714Z.000000000687
32. T. Tański, P. Snopiński, W. Borek, Strength and structure of AlMg3 alloy after ECAP and post-ECAP processing. Mater. Manuf. Processes **32**, 1368–1374 (2017). https://doi.org/10.1080/10426914.2016.1257131
33. Ç. Uğur, G. Turkey, Nano platelets reinforced a composite fabricated through ultra-high frequency induction sintering. Rev. Metal. **57**(1), e188 (2021). https://doi.org/10.3989/revmetalm.188
34. M. Venkatasudhahar et al., Influence of stacking sequence and fiber treatment on mechanical properties of carbon-jute-banana reinforced epoxy hybrid composites. Int. J. Polym. Anal. Charact. **25**, 238–251 (2020). https://doi.org/10.1080/1023666X.2020.1781481
35. R. Vignesh, R. Harichandran, U. Vignesh, M. Thangavel, S.B. Chandrasekhar, Influence of hot extrusion on strain hardening behaviour of graphene platelets dispersed aluminium composites. J. Alloy. Compd. **855**, 157448 (2021). https://doi.org/10.1016/j.jallcom.2020.157448
36. J. Wang, Z. Li, G. Fan, H. Pan, Z. Chen, D. Zhang, Reinforcement with graphene nanosheets in aluminum matrix composites. Scripta Mater. **66**, 594–597 (2012). https://doi.org/10.1016/j.scriptamat.2012.01.012
37. A. Warner, J. Bell, T. Stephenson, Opportunities for new graphitic aluminium metal matrix composite. Mater. Sci. Technol. **14**, 843–850 (1998). https://doi.org/10.1179/mst.1998.14.9-10.843